Distribution of Arrival Times of Air Shower Particles*

P. Bassi,† G. Clark, and B. Rossi
Department of Physics and Laboratory for Nuclear Science, Massachusetts Institute of Technology, Cambridge, Massachusetts
(Received July 13, 1953)

We have studied the instantaneous distribution of particles in extensive air showers at sea level by measuring the relative delays between particles with three liquid scintillation counters. The delays measured were in the range from 5 to 300 mμsec. The sizes of the showers were in the range from 10^5 to 10^6 particles. Using statistical methods of analysis we have found that at a given instant most electrons with energies of ~20 Mev lie in a flat disk of thickness between 1 and 2 meters. The particles which can penetrate at least 20 cm of lead lie in a disk of thickness between 2 and 3 meters. The disk of penetrating particles follows behind the disk of electrons by less then 3 meters.

We measured the projected zenith angles of the axes of individual showers by measuring the delays between widely spaced counters. The standard deviation of a measurement of the sine of the projected zenith angle of a shower was 0.13. The root mean square of the sines of the projected zenith angles was found to be 0.24 ± 0.015. If we assume a $\cos^n\theta$ distribution law for the projected zenith angles we find $n=15\pm1.2$. We determined the spatial orientations of the axes of individual showers by measuring the projections of the zenith angles on two mutually perpendicular planes.

1. INTRODUCTION

PARTICLES in an extensive air shower, generated by a single high-energy particle incident on the top of the atmosphere, may be delayed with respect to one another at the plane of observation because

(1) path lengths may differ as the result of scattering,
(2) velocities may differ,
(3) the axis of the shower may not be perpendicular to the plane of observation.

Several attempts have been made to observe delays due to causes (1) and (2) by recording the times of arrival of air shower particles at detectors. McCusker, Ritson, and Nevin[1] found no particles in air showers which were delayed by more than 1500 mμsec (1500×10^{-9} sec). Mezzetti, Pancini, and Stoppini[2] have shown that the percentage of penetrating particles with delays greater than 100 mμsec is certainly less and probably much less than 15 percent. Delays of penetrating particles have been studied by Officer[3] who found an upper limit of 20 mμsec to the mean delay of particles able to penetrate 10 cm of lead. Jelley and Whitehouse[4] have measured the delays between successive pulses produced in a single large scintillation counter by air showers. They find that 0.6 percent of particles have delays from 30 to 700 mμsec and that the distribution of these delays can be described by an exponential function with half of the delays occurring before a time $\Delta t=100\pm20$ mμsec.

We describe here several experiments which we have carried out with an apparatus sensitive to delays in the range from 5 to 300 mμsec. Our results clarify several features of the instantaneous longitudinal distribution of particles in air showers. In addition they demonstrate that one can determine with fair precision the direction of arrival of air showers from measurements of the delays between widely spaced counters.

At any instant most particles in an air shower are concentrated in a disk-shaped region of space symmetric about the shower axis. This axis is the prolongation of the trajectory of the primary particle. The instantaneous spatial distribution of a certain type of particles will be described by a cylindrically symmetric volume density $\sigma(r, z, t)$, where z is the distance measured along the shower axis, r is the radial distance from the axis, and t is the time (measured from some convenient instant). After the first few radiation lengths from the top of the atmosphere, most of the shower particles will be electrons of about the critical energy traveling at various angles with respect to the shower axis. However, the shape of the spatial distribution will change slowly as the shower propagates downward. By measuring the times of arrival of air shower particles at several counters spread out on the ground, one can, therefore, obtain information about the instantaneous distribution of particles just before the shower struck the ground. In particular, we have measured the thickness of shower disks, the curvature of shower "fronts," the longitudinal distribution of penetrating particles relative to the electrons, and the angular distribution of shower axes.

2. EXPERIMENTAL ARRANGEMENT

Three large liquid scintillation counters, each with a sensitive area of 600 cm², were used both to detect the air showers and to record the times of arrival of the particles. The counters were constructed from the commercial five-gallon drums in which the benzene, used for the scintillation fluid, was delivered. RCA 5819 photomultipliers, selected for high photoelectric efficiency and high gain, were mounted on the tops of the drums by means of adapters as illustrated in Fig. 1. Aluminum foil was spread over the bottoms of the drums in order to increase the amount of light striking

* This work was supported in part by the joint program of the U. S. Atomic Energy Commission and the U. S. Office of Naval Research.
† On leave of absence from the University of Padova, Padova, Italy.
[1] McCusker, Ritson, and Nevin, Nature **166**, 400 (1950).
[2] Mezzetti, Pancini, and Stoppini, Phys. Rev. **81**, 629 (1951).
[3] V. C. Officer, Phys. Rev. **83**, 458 (1951).
[4] J. V. Jelley and W. J. Whitehouse, Proc. Phys. Soc. (London) **66**, 454 (1953).

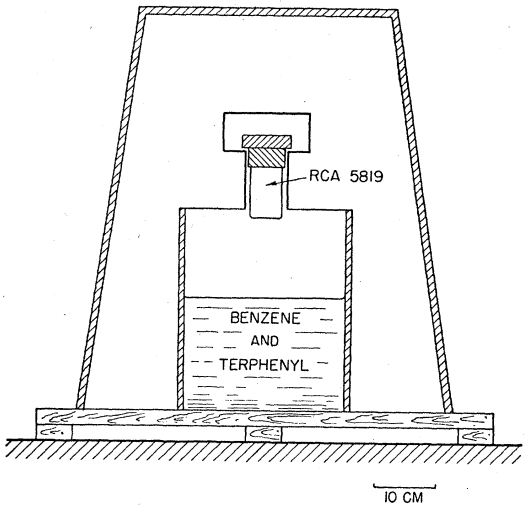

FIG. 1. A schematic diagram of the scintillation counter and protective housing.

the photomultiplier. The counters were filled to a depth of 20 cm with a solution of terphenyl in benzene (3 grams/liter).

A block diagram of the electronic apparatus is shown in Fig. 2. The positive pulses from the last dynodes were conducted by 100-ohm coaxial lines to the central station where they were amplified by fast R-C coupled amplifiers, each with a gain of 500 and a rise time of 20 mμsec. The amplifiers were connected to a crystal diode triple coincidence circuit, and the output of the coincidence circuit was fed into a fast discriminator, employing a secondary emission amplifier tube. Thus, whenever three pulses of sufficient size entered the coincidence circuit within an interval of 300 mμsec, a pulse was generated which triggered the sweep of the oscilloscope. The sweep speed was 100 mμsec/cm. The oscilloscope tube was of the aluminized screen type which permitted long exposures to be made without fogging due to stray light.

The negative pulses from the collecting anodes of the photomultipliers were also conducted by 100-ohm coaxial lines to the central station. At this point artificial delays were introduced between the pulses by suitable lengths of RC-65/U delay line so that the pulses from counters 1, 2, and 3 would appear in proper order in spite of small delays in the arrival of the particles. The pulses were then mixed, amplified (over-all gain of 6000, rise time 15 mμsec), and displayed on the oscilloscope. The oscilloscope traces were photographed with a camera which was automatically advanced one frame for each triple coincidence event. All measurements were made on the oscilloscope record by means of a film projector. We calibrated the sweep with a standard high frequency oscillator and determined that the time scale on the projected image was 1 mm per 5.3 mμsec.

Since much of the experiment was performed with the detectors in the open at temperatures below the freezing point of the scintillation liquid, it was necessary to provide protection for the counters from the weather. We placed the counters on light wooden frames and covered them with inverted ash cans. Electric heating cord was wrapped around the cans and covered with a layer of asbestos for heat insulation.

The total thickness of material between the air and the top surface of the scintillating fluid was approximately 2 g cm^{-2} of steel and brass.

The experiment was performed on the roof of a building at sea level. All the electronic equipment other than the photomultipliers was located in a shelter where daily checks of its performance were made.

We measured the resolving time of the coincidence circuit by determining the amount by which one of the three pulses had to be delayed in order to eliminate the triple coincidence trigger pulse. The resolving time was adjusted so that it was large compared to typical delays which were to be measured.

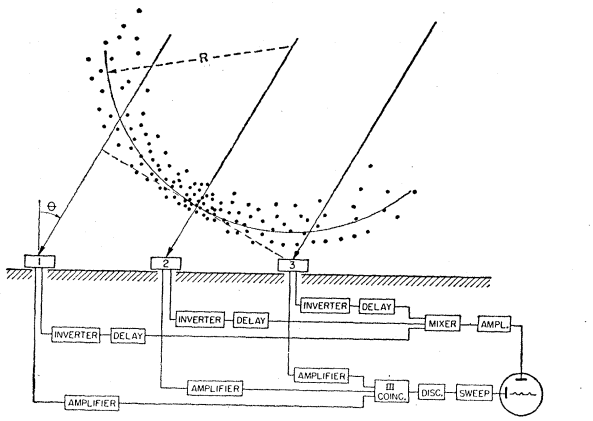

FIG. 2. Block diagram of the apparatus with a schematic representation of an air shower about to strike the counters. The counters are in arrangement II.

The pulses produced by cosmic-ray particles traversing the counters were not much larger than the thermal noise pulses from the photomultipliers. The amplification was fixed so that 300 countable pulses per second were admitted into the coincidence circuit from each counter. The accidental triple coincidence rate was 0.02 hr^{-1}. The efficiencies of the detectors at these settings were then determined by means of a conventional counter telescope arrangement which selected μ mesons traversing the scintillation counters. The efficiencies were ≈ 0.90.

Schematic diagrams of the various arrangements of counters used in our measurements are shown in Fig. 3. In the subsequent discussion it will be convenient to call these arrangements by the numerals indicated in the figure.

The photographic records of several events obtained with arrangement I are reproduced in Fig. 4. Most

triple coincidences with the counters in this vertical arrangement are due to traversals by single μ mesons. We interpret the wide variations in pulse heights as statistical fluctuations due to the small average number of photoelectrons produced in the photomultipliers by a particle of minimum ionization traversing the counters.

We determined the delays between the pulses by measuring the relative positions of the maxima of the three pulses. Approximately 10 percent of the events were rejected because the height of one of the pulses was less than a certain preset minimum height, and 2 percent because one of the pulses was so large as to saturate the amplifier and produce an irregular maximum.

3. THEORY OF DELAY MEASUREMENTS AND METHOD OF ANALYSIS

A. Relations between the Spatial Distribution of Particles, Particle Fluxes, and Delay Distributions

As was mentioned in Sec. 1, the shape of the spatial density distribution $\sigma(r, z, t)$ changes slowly as the

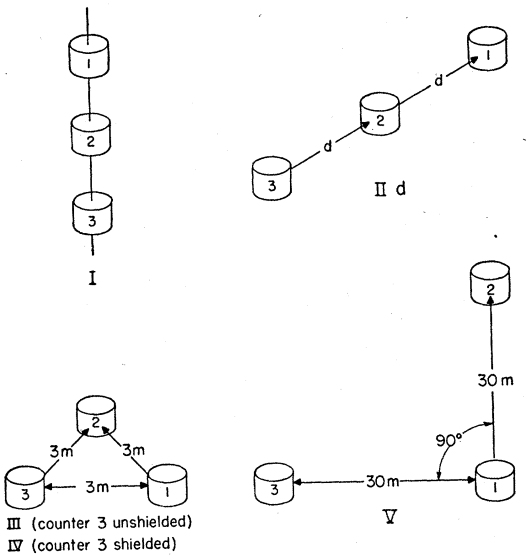

FIG. 3. Schematic diagrams of the arrangements of the counters.

shower propagates along the z axes. Therefore, the time dependence of σ around the time t_0 at a detector located at r_0, z_0 will be related to the z dependence of σ around r_0, z_0 at the time t_0. Specifically,

$$\sigma(r_0, z_0, t)=\sigma(r_0, z', t_0), \tag{1a}$$

where

$$z'=z_0-v(t-t_0), \tag{1b}$$

and v is the velocity of propagation of the shower disk which is practically the velocity of light. $\sigma(r_0, z', t_0)$ is the instantaneous longitudinal density distribution of particles at r_0 at the time t_0.

We shall call $f(r, z_0, t)$ the instantaneous flux of particles through the plane $z=z_0$. Thus $f(r, z_0, t)dtdA$ is the probability that a particle traverses an area dA in the plane $z=z_0$ at a distance r from the axis between the times t and $t+dt$. f and σ are related by the equation

$$f(r, z_0, t)dtdA=\sigma(r, z_0, t)vdtdA=\sigma(r, z', t_0)vdtdA. \tag{2}$$

We shall call $F(r, z_0, t)$ the normalized probability distribution for the time of arrival of the first particle at a counter struck by a shower. Thus $F(r, z_0, t)dt$ is the probability that, if at least one particle traverses a counter of area A at r, z_0, the first particle to do so arrives between the times t and $t+dt$. F and f are related by the equation

$$F(r, z_0, t)dt=\frac{Af(r, z_0, t)dt\exp\left[-A\int_{-\infty}^{t}f(r, z_0, t')dt'\right]}{1-\exp(-m)}, \tag{3}$$

where

$$m=A\int_{-\infty}^{+\infty}f(r, z_0, t)dt$$

is the average number of particles that traverse the counter. The exponential in the numerator represents the probability that no particle has traversed the counter up to the time t. The denominator is the probability that at least one particle traverses the counter.

The shower "front" can now be rigorously defined in terms of F. Suppose $F(r, z_0, t)$ characterizes a shower that arrives at the plane $z=z_0$ near the time t_0. Consider the quantity

$$z_f(r)=\int_{-\infty}^{+\infty}z'F\left(r, z_0, t_0=\frac{z'-z_0}{v}\right)\frac{dz'}{v}. \tag{4}$$

$z_f(r)$ is the expectation value of z at the time t_0 of the first particle that will eventually strike the counter. This quantity depends upon the area of the counter. We call the surface of points $z_f(r)$ the shower front.

B. Interpretation of Correlated Delays

Above the detection apparatus in Fig. 2 we have shown an "instantaneous profile" of a shower about to strike the counters. Individual shower particles are represented by dots. For the purpose of illustration let us imagine that the axis of this shower strikes counter 2, and that it lies in the plane determined by the counters and the zenith. θ is the angle between the axis and the

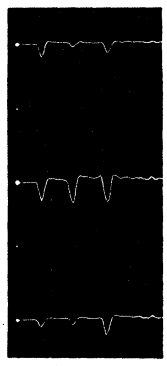

FIG. 4. Photographic records of three shower events showing the pulses from the three scintillation counters.

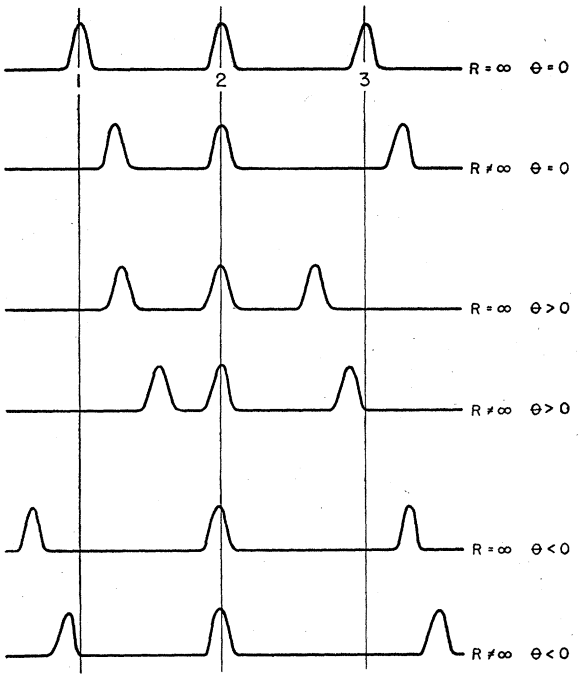

FIG. 5. Idealized diagrams of several types of events showing only the effect of front curvature and axis orientation on the relative positions of the pulses.

vertical. We shall approximate the shape of the front by a spherical surface of radius R.

The sweeps in Fig. 5 illustrate several combinations of pulses corresponding to showers with various values of R and θ, if the thickness of the shower disks and the instrumental fluctuations are negligible. It is important to notice that the effect of a finite value of R is not the same on the time intervals s_{12} (between pulses 1 and 2) and s_{23} (between pulses 2 and 3). Since both pulses 1 and 3 come later with respect to 2 when R is finite than when R is infinite, s_{12} will be decreased and s_{23} will be increased by a curvature of the shower front.

In order to interpret the experimental data we require expressions for s_{12} and s_{23} involving the geometrical properties of showers that we wish to measure, and which take into account the thickness of the shower disks and the instrumental fluctuations. For each event one can compute the relative delays between the arrival times of the first pulses from the three counters. The apparent magnitudes of the delays will depend upon the sweep speed of the oscilloscope which may be subject to small fluctuations. The observed delay will be written as the product of the true delay and a variable factor $(1+a)$ which represents the sweep speed in terms of its average value. Then

$$s_{12}=(1+a)(T_2-T_1+d\sin\theta/v-d^2\cos\theta/2Rv+t_2-t_1+\tau_2-\tau_1), \quad (5a)$$

$$s_{23}=(1+a)(T_3-T_2+d\sin\theta/v+d^2\cos\theta/2Rv+t_3-t_2+\tau_3-\tau_2). \quad (5b)$$

t_1, t_2, and t_3 are the differences between the arrival times of the front at the three counters and the actual arrival times of the first particles at the counters. τ_1, τ_2, and τ_3 represent the random instrumental errors. The t's and τ's are random uncorrelated delays. T_1, T_2, and T_3 are the fixed delays artifically introduced for display purposes. The differences in the arrival times of the front at the various counters due to axis orientation and front curvature give rise to correlated delays which are represented by terms involving d, the distance between counters; θ, the zenith angle; and R the radius of curvature. (Note that $d^2/2R$ is an approximate expression for the sagitta of a spherical segment which is valid if $R\gg d$.)

It can be shown that Eqs. (5) are accurate for any shower provided the axis strikes within a distance from counter 2 small compared to R, and provided θ is the projected zenith angle. Furthermore, the effect of a finite curvature is, in general, at least as great as that represented by the term involving R in Eqs. (5). Thus if one analyzes our data by means of Eqs. (5), one obtains a value of R which is a lower limit on the radius of curvature of shower fronts.

If we add and subtract Eqs. (5) we find

$$(s_{12}+s_{23})=(1+a)(T_3-T_1+2d\sin\theta/v+t_3-t_1+\tau_3-\tau_1), \quad (6a)$$

$$(s_{12}-s_{23})=(1+a)(2T_2-T_1-T_3-d^2\cos\theta/Rv+2t_2-t_1-t_3+2\tau_2-\tau_1-\tau_3). \quad (6b)$$

In the following discussion we shall frequently refer to the statistical concepts of expectation value, dispersion, and standard deviation. In order to make clear the meanings we attach to these concepts and to the symbols we shall use, we state here several definitions.

Let x be a random variable which assumes the values $x_1, \cdots, x_n$. We call

$$E(x)=\frac{1}{n}\sum_{i=1}^{i=n}x_i$$

the expectation value of x. We call

$$D(x)=E\{[x-E(x)]^2\}$$

the dispersion of x. We call $[D(x)]^{\frac{1}{2}}$ the standard deviation of x. Two random variables x and y are said to be independent if

$$E\{[x-E(x)][y-E(y)]\}=0.$$

The following theorems will be used.

Let x and y be independent random variables. Then

$$E(x+y)=E(x)+E(y),$$

$$E(xy)=E(x)E(y),$$

and

$$D[f(x,y)]=[\partial f/\partial x]^2D(x)+[\partial f/\partial y]^2D(y),$$

where the partial derivatives are evaluated for the expectation values of the variables.

We define T_1, T_2, and T_3 so that

$$E(\tau_1)=E(\tau_2)=E(\tau_3)=0.$$

The definition of the shower front that we have given implies that $E(t_1)=E(t_2)=E(t_3)=0$. Then, since a is

independent of the other delay variables and $E(a)=0$,

$$E(s_{12}-s_{23})=2T_2-T_1-T_3-E(d^2\cos\theta/Rv). \quad (7a)$$

As we shall see, all air showers detected in our experiment are strongly collimated in the vertical direction. We can therefore put $\cos\theta=1$ in Eq. (7a). It follows that

$$E_{II}(s_{12}-s_{23})=2T_2-T_1-T_3-(d^2/v)E(1/R). \quad (7b)$$

(Subscripts on the symbols E and D indicate the experimental arrangement used.) The curvature of the shower front has practically no effect on the delays observed with arrangement III. Therefore,

$$E_{III}(s_{12}-s_{23})=2T_2-T_1-T_2. \quad (7c)$$

If we combine Eqs. (7b) and (7c) we find that

$$E(1/R)=(v/d^2)[E_{III}(s_{12}-s_{23})-E_{II}(s_{12}-s_{23})]. \quad (8)$$

Consider now the dispersions of the measured quantities. Anticipating the experimental results, we state that we can neglect the term involving $1/R$. Thus we can write

$$D(s_{12}+s_{23})=D(2d\sin\theta/v)+D(t_3)+D(t_1)+D(\tau_3)+D(\tau_1)+(T_3-T_1)^2D(a), \quad (9a)$$

and

$$D(s_{12}-s_{23})=4D(t_2)+D(t_1)+D(t_3)+4D(\tau_2)+D(\tau_1)+D(\tau_3)+(2T_2-T_1-T_3)^2D(a). \quad (9b)$$

$D(a)$ can be estimated from measurements with arrangement I. As we mentioned earlier, most of the triple coincidences with arrangement I are produced by single μ mesons. Thus

$$D(t_1)=D(t_2)=D(t_3)=0.$$

We shall assume in our analysis that the instrumental fluctuations are the same for all three pulses, i.e.,

$$D(\tau_1)=D(\tau_2)=D(\tau_3)=D(\tau).$$

If we omit the term $D(2d\sin\theta/v)$, we have from Eqs. (9a) and (9b)

$$D_I(s_{12}+s_{23})=2D(\tau)+(T_3-T_1)^2D(a), \quad (9c)$$

and

$$D_I(s_{12}-s_{23})=6D(\tau). \quad (9d)$$

In Eq. (9b) the term $(2T_2-T_1-T_2)^2D(a)$ can be neglected because we have adjusted the instrumental delays so that $(2T_2-T_1-T_3)\approx 0$. Then, from Eqs. (9c) and (9d) it follows that

$$D(a)=[D_I(s_{12}+s_{23})-\tfrac{1}{3}D_I(s_{12}-s_{23})]/(T_3-T_1)^2. \quad (10)$$

In the case of the measurements with arrangement II we will put

$$D(t_1)=D(t_2)=D(t_3)=D(t).$$

Thus,

$$D_{II}(s_{12}+s_{23})=(4d^2/v^2)D(\sin\theta)+2D_{II}(t)+2D(\tau)+(T_3-T_1)^2D(a), \quad (9e)$$

$$D_{II}(s_{12}-s_{23})=6D_{II}(t)+6D(\tau), \quad (9f)$$

where we have again neglected the term $(2T_2-T_1-T_3)^2D(a)$. From Eqs. (9e) and (9f) it follows that

$$(4d^2/v^2)D(\sin\theta)=D_{II}(s_{12}+s_{23})-\tfrac{1}{3}D_{II}(s_{12}-s_{23})-(T_3-T_1)^2D(a). \quad (11)$$

C. Interpretation of Uncorrelated Delays

One can estimate the thickness of the shower disks by combining the measurements of $D(s_{12}-s_{23})$ made with arrangements I and II or III. From Eqs. (9d) and (9f) one obtains

$$D_{IId}(t)=\tfrac{1}{6}[D_{IId}(s_{12}-s_{23})-D_I(s_{12}-s_{23})]. \quad (12a)$$

Also, since d is small in arrangement III,

$$D_{III}(t)=\tfrac{1}{6}[D_{III}(s_{12}-s_{23})-D_I(s_{12}-s_{23})]. \quad (12b)$$

Electrons are the particles primarily responsible for the discharge of the unshielded counters in a shower. Therefore, $D_{IId}(t)$ and $D_{III}(t)$ are the dispersions of arrival times of first electrons averaged over ranges of shower sizes and over ranges of distances from the shower axes. $v[D_{IId}(t)]^{\frac{1}{2}}$ and $v[D_{III}(t)]^{\frac{1}{2}}$ are measures of the thickness of the shower disks (see Section IVC).

It is possible to shield a counter so that it can be discharged only by penetrating particles. If one compares the arrival times of pulses from a shielded counter and from unshielded counters one can obtain information about the difference between the arrival times of the front of penetrating particles and of the front of electrons. We shall call this difference Λ_{ep}. If counter 3 is shielded (arrangement IV) and if t_1, t_2, and t_3 are all measured with respect to the front of electrons, then

$$E_{IV}(t_1)=E_{IV}(t_2)=0; \quad E_{IV}(t_3)=\Lambda_{ep}.$$

From Eq. (6b) we deduce that

$$E_{IV}(s_{12}-s_{23})=2T_2-T_1-T_3+\Lambda_{ep}. \quad (7d)$$

If one compares Eqs. (7c) and (7d) one then finds

$$\Lambda_{ep}=E_{IV}(s_{12}-s_{23})-E_{III}(s_{12}-s_{23}). \quad (13)$$

$v[D_{IV}(t_3)]^{\frac{1}{2}}$ is a measure of the thickness of the disk of penetrating particles. We shall assume that

$$D_{IV}(t_1)=D_{IV}(t_2)=D_{III}(t).$$

We can then write

$$D_{III}(s_{12}-s_{23})=6D_{III}(t)+6D(\tau),$$

and

$$D_{IV}(s_{12}-s_{23})=5D_{III}(t)+D_{IV}(t_3)+6D(\tau)$$

from which one obtains

$$D_{IV}(t_3)=D_{IV}(s_{12}-s_{23})-\tfrac{5}{6}D_{III}(s_{12}-s_{23})-\tfrac{1}{6}D_I(s_{12}-s_{23}). \quad (14)$$

The advantage of using the delay differences instead of the sums is, of course, that the differences are not affected by fluctuations in the sweep speed.

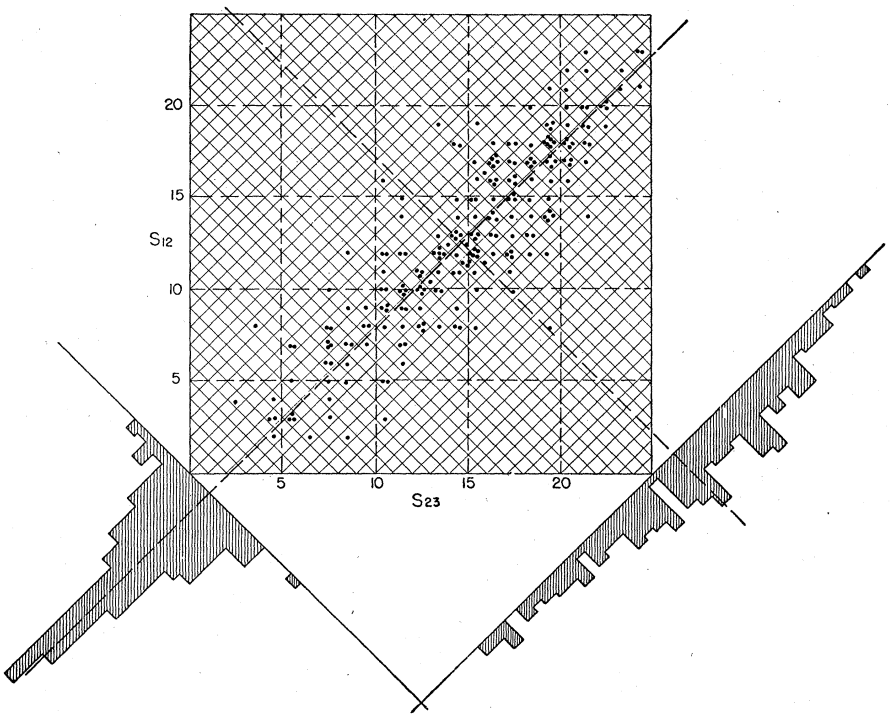

FIG. 6. Graphical summary of data obtained with arrangement II 30. Each shower event is represented by a dot with Cartesian coordinates s_{12}, s_{23}. The scales are 5.3 mμsec per division. The location of the origin is arbitrary.

D. Graphical Presentation of Data; Orientation of Shower Axes

Figure 6 illustrates a way of plotting the experimental data which clarifies the statistical problems involved in the analysis. We recorded a large number of shower events with a certain disposition of counters, and for each event we obtained the measured quantities s_{12} and s_{23}. Each event is then represented by a point with Cartesian coordinates s_{12} and s_{23} (Fig. 6). The points for a typical experimental run with arrangement II 30 are distributed in an approximately elliptical region whose major axis is inclined at 45°. From Eqs. (5) it is clear that if R were infinite and the uncorrelated delays negligible, then all the points would lie on the 45° line. (Note that if $T_2-T_1\neq T_3-T_2$, the major axis does not pass through the origin.) The breadth of the elliptical region is related to the thickness of the shower disks. The projected distribution of points on the major axis is related to the distribution of zenith angles of shower axes. In Fig. 6 two histograms have been plotted which represent the projected distributions of points on the 45° and 135° lines. The 45° histogram is the histogram of $1/\sqrt{2}(s_{12}+s_{23})$; the other is the histogram of $1/\sqrt{2}(s_{12}-s_{23})$.[5]

[5] These assertions can be demonstrated in the following way: Represent an experimental point by the vector $\mathbf{X}=(s_{12}, s_{23})$. Consider the unit vectors $\mathbf{U}_+=1/\sqrt{2}(1, 1)$ and $\mathbf{U}_-=1/\sqrt{2}(-1, 1)$ parallel to the 45° and 135° lines, respectively. Then the projection of $\mathbf{X}$ on the 45° line is

$$\mathbf{X}\cdot\mathbf{U}_+=1/\sqrt{2}(s_{12}+s_{23})$$

and on the 135° line is

$$\mathbf{X}\cdot\mathbf{U}_-=1/\sqrt{2}(s_{12}-s_{23}).$$

The coordinates of the "center of gravity" of the delay distribution are

$$\bar{s}_{12}=E(s_{12}); \quad \bar{s}_{23}=E(s_{23}).$$

With the counters close together in arrangement III the center of gravity corresponds to the point representing the simultaneous discharge of the three counters. With the counters in arrangement II d, the increase in the dispersion of correlated delays due to variations in the zenith angles produces an elongation of the distribution of points. In addition, the effect of any general curvature of shower fronts will be to move the center of gravity down and to the right. The displacement of the center of gravity will be proportional to the separation, d, of the counters.

One can determine the projected zenith angle, within certain errors by measuring the delay between the discharges of two widely separated counters. With three counters placed at the vertices of a right triangle as in arrangement V, one can therefore measure the projection of the zenith angle on two mutually perpendicular planes and from these projected angles obtain the spatial orientation of the axis. The accuracy of this method depends, of course, on the relative magnitudes of the delays due to uncorrelated fluctuations and axis orientation.

With arrangement V the plot of s_{12} *vs* s_{23} for a large number of showers takes on a different appearance and meaning (Fig. 10). The experimental points are distributed in a circular region whose center of gravity corresponds to a vertical shower. The plotted dis-

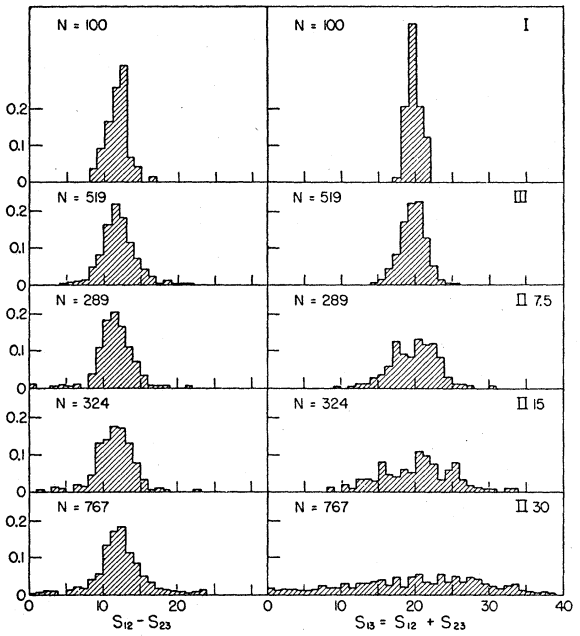

FIG. 7. Histograms of the sums and differences of the observed relative delays. The scale on the horizontal axes is 5.3 mμsec per division. The histogram intervals are 5.3 mμsec. The areas of the histograms are normalized to 1. N indicates the number of recorded events.

tribution is the projection of the spherical distribution of shower axes onto the equatorial plane. The azimuth and altitude (zenith angle) of each shower axis can therefore be determined directly from the plot. An annular ring with radii S_a and S_b contains points representing axes with zenith angles in the range

$$\arcsin(S_a v/d) < \Theta < \arcsin(S_b v/d).$$

If one measures the frequency of counts within successive annular rings, one can determine the distribution in zenith angle of shower axes.

Although the use of this graphical representation is not absolutely necessary in the interpretation of our data, we have found that it clarifies the statistical problems and facilitates the numerical evaluation of the experimental results.

4. EXPERIMENTAL RESULTS

A. Instrumental Fluctuations

Sweep speed fluctuations result from slow changes in circuit constants and operating conditions and are not random. It is not, possible, therefore, to subtract the dispersion due to sweep speed fluctuations from the measured dispersions in a rigorous way. However, we have made an estimate of $[D(a)]^{\frac{1}{2}}$ using Eq. (10) and the data collected in several runs with arrangement I over a period of twenty days. We found

$$[D(a)]^{\frac{1}{2}} = 0.02,$$

which is equivalent to 5 mμsec on a length of sweep equal to $T_3 - T_2 = T_2 - T_1 = 250$ mμsec.

The other instrumental fluctuations are random and uncorrelated. They arise partly from fluctuating delays in the counters and electronic circuits, and mostly from errors in the measurement of the positions of the pulses. Figures 7–I are histograms of $s_{12}-s_{23}$ and $s_{12}+s_{23}$ obtained in one short run with arrangement I in which the apparatus responds primarily to single penetrating particles. Over the short period of time occupied by this run $D(a) \approx 0$. From Eqs. (9c) and (9d) we see that we should find

$$D(s_{12}-s_{23})/D(s_{12}+s_{23}) = 3.$$

From several short runs we find for the above ratio a value of 2.3 ± 0.6 which agrees roughly with the expected ratio. Assuming the dispersions of τ_1, τ_2, and τ_3 to be equal, we find

$$[D(\tau)]^{\frac{1}{2}} = [\tfrac{1}{6} D(s_{12}-s_{23})]^{\frac{1}{2}} = 3.0 \text{ mμsec}.$$

B. Determination of a Lower Limit on the Radius of Curvature of Shower Fronts

We measured $E_{\text{II }30}(S_{12}-s_{23})$ and $E_{\text{III}}(s_{12}-s_{23})$. Using Eq. (8) we evaluated $E(1/R)$. As a precaution against slow instrumental changes, we made measurements alternately with the two arrangements. Figure 8 is a plot of the values of $E(s_{12}-s_{23})$ for successive experimental runs. No large systematic difference was found in the results obtained with arrangements II 30 and III. The combined data from the two runs with arrangement II 30 and the three runs with arrangement III were used in computing $[E(1/R)]^{-1}$. We found

$$[E(1/R)]^{-1} = 2600 \text{ m}.$$

If we consider the statistical errors, the lower limit on the radius of curvature of the fronts of showers detected with arrangement II 30 is 1300 m.

C. Thickness of Shower Disks

Since, as we have seen, the fronts are nearly plane, we can find $D(t)$ from Eqs. (12) using measured values

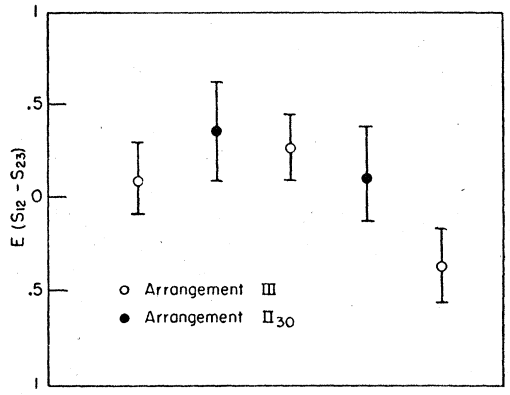

FIG. 8. Plot of the expectation values of $s_{12}-s_{23}$ obtained from successive experimental runs with arrangements II 30 and III.

TABLE I. Summary of statistical results obtained with various arrangements of counters.

Arrangement of counters	No. of showers observed	$[D(S_{12}-S_{23})]^{\frac{1}{2}}$ (mμsec)	$[D(S_{12}+S_{23})]^{\frac{1}{2}}$ (mμsec)	$[D(t)]^{\frac{1}{2}}$ (mμsec)	$v[D(t)]^{\frac{1}{2}}$ meters	$[D_{IV}(t_3)]^{\frac{1}{2}}$ (mμsec)	$v[D_{IV}(t_3)]^{\frac{1}{2}}$ meters	$D(S_{12}+S_{13})-\frac{1}{3}D(S_{12}-S_{13})$ $\times 10^{-18}$ sec^2
I	300	7.4±0.4	4.8±0.2	...	...	...	...	...
III	519	12.1±0.4	9.0±0.3	4.0±1	1.2±0.3	...	...	...
II 7.5	289	13.4±0.5	17.6±0.7	4.5±1	1.35±0.3	...	...	250±26
II 15	324	16.2±0.6	26.5±1.0	5.8±1	1.7±0.3	...	...	615±50
II 30	767	21.0±0.5	50.3±1.5	8.0±1	2.4±0.3	...	...	2383±150
IV	...	14.1±0.5	...	...	...	8.2±2.0	2.5±0.6	...

of $D_I(s_{12}-s_{23})$, $D_{IId}(s_{12}-s_{23})$, and $D_{III}(s_{12}-s_{23})$. The histograms in Fig. 7 summarize our data. In Table I we have listed the values of $[D(s_{12}-s_{23})]^{\frac{1}{2}}$ and the numbers of events used in the evaluations. We have also listed the corresponding values of $v[D(t)]^{\frac{1}{2}}$ which, as we shall discuss in more detail below, are indications of the thickness of the shower disks. It should be noted that $[D(t)]^{\frac{1}{2}}$ increases with d.

If we assume the validity of the Molière radial distribution function and use a method similar to that of Blatt,[6] we estimate that the range of sizes of showers detected with these counter arrangements is from 10^5 to 10^6 particles. The median size of showers detected with arrangement IId increases with d. The ratio of median shower sizes for arrangements II 7.5, II 15, and II 30 are approximately 1:3:9.

In order to draw from the measurements a clear conclusion as to the thickness of shower disks, we must consider in detail the significance of the quantity $[D(t)]^{\frac{1}{2}}$. Let us represent the instantaneous fluxes of electrons through all these counters by the single function $f_e(t)$. Then $D(t)$ is the dispersion of the corresponding first particle time distribution $F_e(t)$. According to Eq. (3), F_e differs more and more from $(1/m)f_e$ as the average number of electrons traversing a counter increases. Our method of selecting showers insures that the average number of traversals is close to one. However, in order to form an idea of the relation between the two functions, we evaluated $F_e(t)$ for a selected form of $f_e(t)$ and for several values of the average number of traversals m. We assume that

$$f_e(t)=\exp(-t/\lambda_e), \quad t>0$$
$$=0, \quad t<0.$$

and values of m from 0.5 to 3. The results of these calculations are presented in Fig. 9. For the sake of comparison we have plotted a dashed line to represent $(1/m)f_e(t)$. The dispersion of F_e is clearly smaller than the dispersion of f_e. One must expect, therefore, a significant difference between the dispersion in arrival times of first particles and the dispersion in arrival times of all particles. However, our measurements are not sufficiently accurate to insure that we measure only first particles. In practice, when two particles traverse a counter within a time interval comparable to our instrumental fluctuations, they produce a deflection of the oscilloscope beam which looks like a single pulse whose maximum occurs at a time corresponding, more or less, to the average of the two arrival times. Thus the dispersion that we actually measure is the dispersion of a function which lies between f_e and F_e.

Scattering of the electrons in the last radiation length above the counters is sufficient in itself to account for the thickness of the shower disks as can be seen from the following argument: the lower limit of the energy of the electrons detected by the counters is about 20 Mev. The mean energy is about 50 Mev. The root-mean-square angle of scattering in the last radiation length for electrons with a residual energy of 50 Mev is approximately 0.2 radian. In one radiation length in air at sea level this scattering results in an increase of path length of about 3 m, which corresponds to a delay of 10 mμsec. If the electrons are produced in a circular region of radius 30 m at a distance of 300 m above the plane of observation, then this amount of scattering would result in an almost flat shower disk of thickness 3 m, which is roughly the same as the measured values of $v[D(t)]^{\frac{1}{2}}$.

The apparent increase of the disk thickness with d may be due to the increase of the mean shower size with d. It seems unlikely that the effect could be due to a general thickening of shower disks with increasing distance from the shower axis, since this would almost certainly cause the fronts to be curved contrary to the observation we have reported.

The small thickness of the electron shower disk points to a conclusion regarding the mechanism of production of the shower. Certainly many of the electrons present in the disk at sea level are descendents of the neutral π mesons produced in the first nuclear interaction of the primary particle near the top of the atmosphere. If an appreciable fraction of the electrons at sea level come from later generations in the nucleonic cascade, then the N particles which link these later generations with the first nuclear interaction must be of very high energy since their descendent electrons are observed to be not greatly delayed with respect to the first electrons which arrive at sea level. Specifically, the energy of a proton which is delayed by 10 mμsec (3 m) with respect to a particle traveling with the velocity of light over a length of 100 g cm^{-2} at sea level is 12 Bev, and at 14 km is 27 Bev. These values are,

[6] J. Blatt, Phys. Rev. **75**, 1584 (1949).

therefore, conservative lower limits on the energies of the nucleon links.

D. Average Projected Zenith Angle of Shower Axes

From measurements of $D(s_{12}+s_{23})$ and $D(s_{12}-s_{23})$ with arrangement IId one can determine $D(\sin\theta)$ [see Eq. (11)] if the term involving $D(a)$ can be neglected. As we observed before, an exact evaluation of $D(a)$ is impossible. However, from the measurements reported in IVA it is possible to estimate that the magnitude of $(T_3-T_1)^2D(a)$ is not greater than 100×10^{-18} sec^2. From the numbers quoted in column 9 of Table I it is clear that this quantity is small compared to the values of $D_{\mathrm{II}d}(s_{12}+s_{23})-\frac{1}{3}D_{\mathrm{II}d}(s_{12}-s_{23})$ obtained with $d=7.5$, 15 and 30 m. Certainly for $d=30$ m the error introduced by the sweep speed fluctuations is negligible. For $d=30$ m we deduce

$$D_{\mathrm{II}\,30}(\sin\theta)=0.059\pm0.004$$

for the dispersion of the sine of the projected zenith angles of shower axes.

In order that this result may be compared with previous experiments and with theoretical predictions, we have assumed that the distribution of projected zenith angles follows a $\cos^n\theta$ law, and we have calculated the value of n which would give the observed dispersion of $\sin\theta$. It can be shown that

$$D(\sin\theta)=\int_0^{\pi/2}\sin^2\theta\cos^n\theta d\theta\Big/\int_0^{\pi/2}\cos^n\theta d\theta=1/n+2.$$

From this equation and the measured value of $D(\sin\theta)$ we find

$$n=15\pm1.2.$$

It should be emphasized that these results on the projected zenith angle distribution do not depend on the detailed interpretation of the first particle dispersion which we gave in IVC.

Jánossy[7] has calculated the zenith angle distribution in approximation A for showers of 10^5 and 10^6 particles initiated by photons near the top of the atmosphere. He finds $n=16$. We have calculated the distribution in approximation B using graphical integrations, and we found the same value of n.

E. Determination of the Orientations of Shower Axes; Distribution of the Zenith Angles of Showers

We shall now evaluate the error in a measurement of the projected zenith angle of a shower axis using two counters. From Eq. (5) it can be seen that the principal effect of fluctuations in a on $D(s_{12})$ is through the term involving the artificial delays between pulses, since T_2-T_1 is large compared to $E(d\sin\theta/v+t_2-t_1+\tau_2-\tau_1)$. Now, $T_2-T_1=250$ mμsec. Since $[D(a)]^{\frac{1}{2}}=0.02$, the error introduced by this term is of the order of 6 mμsec. From $D_{\mathrm{II}d}(s_{12}-s_{23})$ we can evaluate the errors due to disk thickness and instrumental fluctuations. We find $[D(t+\tau)]^{\frac{1}{2}}=12$ mμsec. Therefore, the standard deviation of a measurement of s_{12} due to instrumental fluctuations and disk thickness is

$$[2D(t+\tau)+(T_2-T_1)2D(a)]^{\frac{1}{2}}=13\ \mathrm{m}\mu\mathrm{sec}.$$

This results in an error in the determination of the sine of the projected zenith angle amounting to 0.13. Using counters 1 and 3, the error in the sine is 0.15, which is greater than with counters 1 and 2 because the greater sweep length emphasizes fluctuations in sweep speed. The fundamental limitation on the accuracy of angle measurements made by this method is, of course, the dispersion in arrival times of first particles which in our case accounts for an error of 0.12 in the determination of $\sin\theta$.

Using arrangement IV we measured the spatial orientation of 350 shower axes. The data is summarized in Fig. 10. The plot illustrates clearly the strong vertical collimation of shower axes. Figure 11 is a histogram of the spatial zenith angles computed from Fig. 10 by counting the frequencies of points within successive annular rings.

F. Delays of Penetrating Particles

The delays of penetrating particles were measured with arrangement IV in which counter 3 was shielded on the top and sides by lead 20 cm thick. In addition, counter 3 was located under a concrete roof 60 g cm^{-2} thick.

From our data we computed $E_{\mathrm{IV}}(s_{12}-s_{23})$. $E_{\mathrm{III}}(s_{12}-s_{23})$ was obtained with all three counters unshielded in arrangement III. If we apply Eq. (13) we

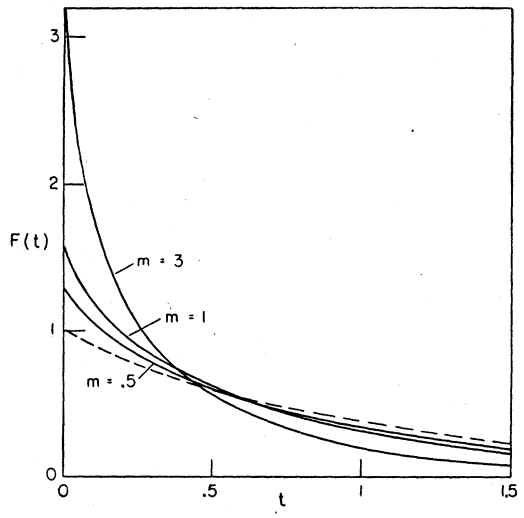

FIG. 9. Comparison of $F_e(t)$ (solid lines) and $f_e(t)$ (dashed line) for several values of m.

[7] Jánossy, *Cosmic Rays* (Oxford University Press, London, 1950), second edition, p. 337.

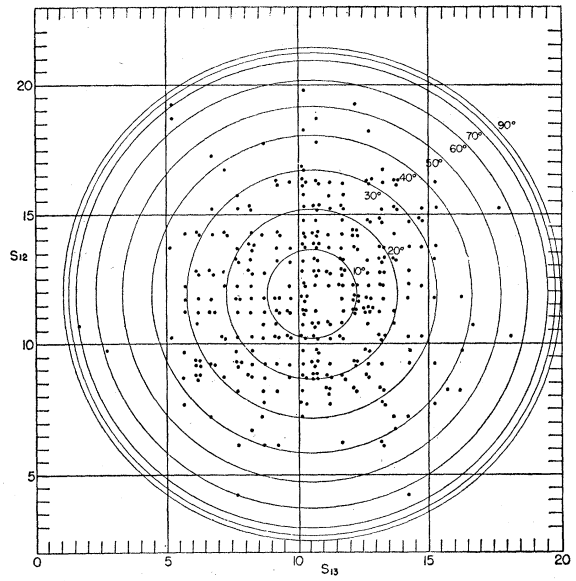

FIG. 10. Graphical summery of the data on the spatial orientation of shower axes obtained with arrangement V. The scales are 5.3 mμsec per division. The zenith angles of the shower axes are indicated by the concentric circles.

find the difference in the arrival times of the front of electrons and the front of penetrating particles to be

$$\Lambda_{ep}=9.5 \text{ m}\mu\text{sec.}\dagger$$

If we combine $D_{\text{IV}}(s_{12}-s_{23})$ and $D_{\text{III}}(s_{12}-s_{23})$ according to Eq. (14) we find

$$[D_{\text{IV}}(t_3)]^{\frac{1}{2}}=8\pm 2 \text{ m}\mu\text{sec.}$$

The values of Λ_{ep} and $[D_{\text{IV}}(t_3)]^{\frac{1}{2}}$ quoted here are subject to a statistical bias introduced by the coincidence circuit which accepts an event only if the three pulses occur within an interval of 300 mμsec. These results, therefore, apply to penetrating particles that are delayed by less than 300 mμsec.

The experiments of Cocconi, Tongiorgi, and Greisen[8] demonstrated that penetrating particles are present in air showers at sea level to the extent of approximately 2 percent of the total ionizing radiation. The small absorption suffered by this penetrating component in air and in lead and iron indicated that it consists mostly of μ mesons. Recent work of McCusker[9] has shown that approximately 35 percent of the penetrating radiation in showers at sea level consist of N particles. Since the shielding over counter 3 in our measurements absorbs at least 50 percent of the N component incident from the atmosphere, it is probable that most of the penetrating particles detected in our experiment were μ mesons. The observed delay in the arrival of the penetrating particle front is consistent with this picture as can be seen from the following argument: in Fig. 12 we have evaluated the delays of μ-mesons and of protons of various $\gamma=E/mc^2$ with respect to particles traveling with the speed of light on different paths in the atmosphere. The numbers in parentheses indicate the initial γ's at 20 km and the final γ's at sea level. We can estimate the delay of the penetrating particle front by adding $[D(t)]^{\frac{1}{2}}$ (a measure of the delay of the electron front) to Λ_{ep} (the delay of the penetrating particle front relative to the electron front). This delay is 13 mμsec. If we assume that the average energy of μ mesons in showers at sea level is between 2 and 4 Bev, than the altitude of production corresponding to the observed delay is between 5 and 20 km. If the average energy of nucleons in showers were between 2 and 4 Bev, the altitude of production corresponding to the observed delay would be between 30 m and 120 m. For this reason we can exclude nucleons as a main component of the penetrating particles we detected. The height of production we have deduced for μ mesons is consistent with the usual picture of air showers.

5. CONCLUSIONS

If we add our results to the description of air showers which has been deduced from other experiments, one can construct the following picture of an extensive air shower. A primary proton striking an air nucleus at an altitude near 20 km initiates a cascade of nuclear interactions. The neutral π mesons produced in these interactions give rise to the electromagnetic component; the charged π mesons give rise to the μ mesons. Because a large fraction of the electron component observed at

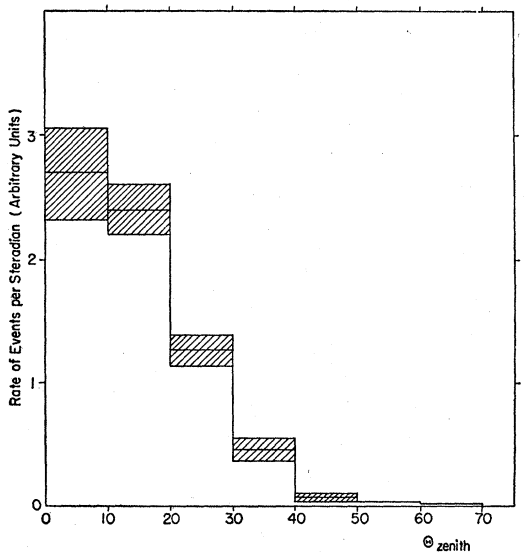

FIG. 11. Histogram of the frequency of showers with zenith angle Θ per unit solid angle as a function of Θ.

† Of course, Λ_{ep} does not represent the difference between the mean arrival times of electrons and penetrating particles, because the numbers, m, of electrons and penetrating particles are not the same (see discussion in Sec. 3C).

[8] Cocconi, Cocconi-Tongiorgi, and Greisen, Phys. Rev. **75**, 1063 (1949).

[9] C. B. A. McCusker, Proc. Phys. Soc. (London) **A63**, 1240 (1950).

sea level probably comes from the neutral π mesons generated in the first few interactions of the nucleonic cascade, a large production of electronic radiation at lower altitudes by low-energy nucleons would result in an increase in the thickness of the electron shower disk due to the kinematic delays of the nucleons. From the observed thickness, which can be accounted for on the basis of scattering alone, we deduce a conservative lower limit of $\sim$20 Bev on the energy of nucleons which are responsible for the production of an appreciable fraction of the electrons we observe at sea level.

Charged π mesons produced in the first few nuclear interactions partly interact and partly decay into μ mesons. From the delay between the front of penetrating particles and the front of electrons, we conclude that the main production of the μ mesons observed at sea level occurs at an altitude of approximately 10 km.

When an air shower reaches sea level most electrons in the shower are concentrated in a flat disk of radius 60 m and thickness between 1 and 2 m. The disk of particles which can penetrate 20 cm of lead has the same lateral dimensions, a thickness between 2 and 3 m, and its front follows behind the front of electrons by about 3 m. The penetrating particles we detected consisted mostly of μ mesons.

The dispersion of the sines of the projected zenith angles of shower axes is 0.059 which, assuming a $\cos^n\theta$ law, corresponds to $n=15$. The orientation of individual shower axes can be determined by delay measurements. The error (standard deviation) in our determination of the sine of the projected zenith angle of an individual shower axis is 0.13. The error is due principly to the thickness of the shower disk.

In conclusion we wish to express our gratitude to Professor W. L. Kraushaar for the design of the fast amplifiers, and to Dr. S. Olbert for valuable discussions of several phases of this work. We thank Dr. J. V. Jelley and Dr. W. Whitehouse for sending us the results of their experiments before publication. We also thank Mr. W. Smith and Mr. J. Strickland for their assistance in the construction and operation of the equipment.

One of us (P.B.) acknowledges the financial assistance he received from the Fulbright Program and from the Associazione Industrali di Trieste.

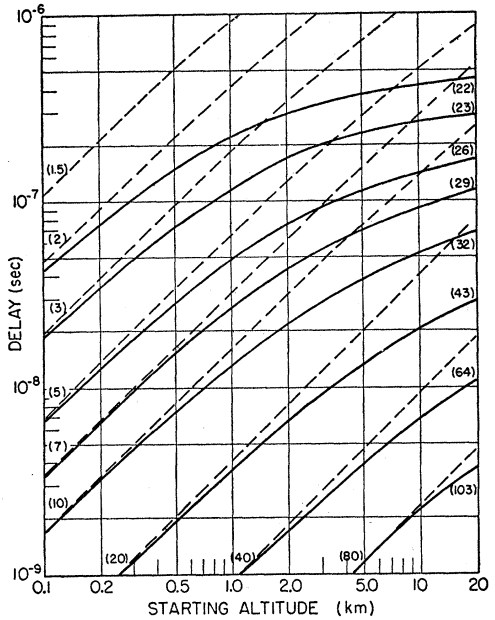

FIG. 12. Plot of the delays of protons (dashed lines) and μ mesons (solid lines) relative to particles traveling with the speed of light over various paths in the atmosphere. The numbers in parentheses indicate the values of $\gamma=E/mc^2$ at sea level and at 20 km. One finds the delay of a particle, which reaches sea level with a certain γ_0, over a path from altitude h_0 to sea level, by reading from the graph the value of the delay which corresponds to h_0 along the curve with residual $\gamma=\gamma_0$.

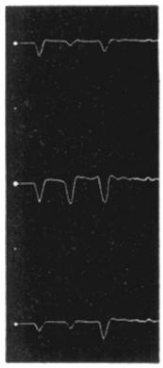

FIG. 4. Photographic records of three shower events showing the pulses from the three scintillation counters.